Schizosaccharomyces pombe KAT5 contributes to resection and repair of a DNA double strand break

Tingting Li[1], Ruben C. Petreaca[1&2] and Susan L. Forsburg[1&]*

[1]Program of Molecular and Computational Biology, University of Southern California, Los Angeles CA 90089-2910

[2]Department of Molecular Genetics, Ohio State University, Marion OH 43302

*Corresponding author at Forsburg@usc.edu

Keywords: fission yeast, DSB repair, KAT5, Mst1, resection

Abstract

Chromatin remodeling is essential for effective repair of a DNA double strand break. KAT5 (*S. pombe* Mst1, human TIP60) is a MYST family histone acetyltransferase conserved from yeast to humans that coordinates various DNA damage response activities at a DSB, including histone remodeling and activation of the DNA damage checkpoint. In *S. pombe*, mutations in *mst1+* causes sensitivity to DNA damaging drugs. Here we show that Mst1 is recruited to DSBs. Mutation of *mst1+* disrupts recruitment of repair proteins and delays resection. These defects are partially rescued by deletion of *pku70*, which has been previously shown to antagonize repair by homologous recombination. These phenotypes of *mst1* are similar to *pht1-4KR*, a non-acetylatable form of histone variant H2A.Z, which has been proposed to affect resection. These data suggest that Mst1 functions to direct repair of DSBs towards homologous recombination pathways by modulating resection at the double strand break.

Introduction

The DNA damage response choreographs multiple cellular activities such as lesion detection, activation of the DNA damage checkpoint, break repair, and recovery (Langerak and Russell 2011). Chromatin remodeling is central to the faithful execution of these processes, requiring the coordination of histone modifiers, remodelers, and chromatin assembly factors (rev. in (Bakkenist and Kastan 2015; Miller and Jackson 2012; Price and D'Andrea 2013; Ransom, Dennehey, and Tyler 2010; Rossetto et al. 2010). Acetylation of histone H4 is one marker associated with chromatin remodeling at a double strand break (DSB), a potentially lethal form of DNA damage. There is good evidence that histone H4 acetylation is linked to radioresistance and the repair response, possibly by facilitating chromatin mobilization (e.g., (Bird et al. 2002; Downs et al. 2004; Murr et al. 2005; Song, McCann, and Brown 2008; Tamburini and Tyler 2005; Xu et al. 2012)).

The MYST family of histone acetyltransferases (HATs) is defined by a distinct catalytic domain, and its members are implicated in histone acetylation at DSBs (Thomas and Voss 2007; Utley and Côté 2003). KAT5 is

the most highly conserved HAT of this family, known as Mst1 in *S. pombe,* Esa1 in *S. cerevisiae*, and TIP60 in mammals (reviewed in (Avvakumov and Côté 2007; Pillus 2008)). The gene is essential for viability in all species, because in addition to its role in DSB repair it performs other functions such as transcriptional regulation, heterochromatin assembly and centromere assembly (Doyon and Côté 2004; Ghobashi and Kamel 2018; Gómez et al. 2008; Nugent et al. 2010; Pillus 2008). In humans, TIP60 has also been identified as a tumor suppressor (rev. (Sapountzi, Logan, and Robson 2006; Voss and Thomas 2009) and is a therapeutic target (rev. in (Judes et al. 2015).

KAT5 contains a chromodomain in addition to its HAT domain, which suggests that it binds methylated histones (rev. in (De La Cruz et al. 2005; Utley and Côté 2003)). KAT5 functions in the context of a large protein complex called NuA4, and acetylates numerous substrates including histones H2A, H3, and H4, and the histone variants H2A.X and H2A.Z (Allard et al. 1999; Babiarz, Halley, and Rine 2006; Galarneau et al. 2000; Keogh et al. 2006; Kimura and Horikoshi 1998; Smith et al. 1998). Evidence from human cells has shown that KAT5 can acetylate non-histone proteins as well, including the checkpoint kinase ATM and the tumor suppressor TP53 (X. Jiang et al. 2006; M.-Y. Kim et al. 2007; Leduc et al. 2006; Naidu, Lakhter, and Androphy 2012; Ortega-Atienza et al. 2016; Sun et al. 2005; Sykes et al. 2006; Y. Tang et al. 2006). Importantly, NuA4 also associates with the Swr1 chromatin remodeler that is required for exchange of histone H2A with the variant H2A.Z (Keogh et al. 2006; Kobor et al. 2004; Krogan et al. 2004; Zhou et al. 2010).

Evidence from both yeast and humans shows that the NuA4 complex is recruited to DSBs by multiple binding partners including phosphorylated H2A(X) (Downs et al. 2004), methylated histone H4K20 (Jacquet et al. 2016), methylated histone H3K36 (Li and Wang 2017), methylated histone H3K9 via the KAT5 chromodomain (Sun et al. 2005; Sun et al. 2009, Ayrapetov et al. 2014), and interaction with Nbs1, a component of the end-binding resection complex MRN (Xue Cheng et al. 2018). In fission yeast, physical association between KAT5/SpMst1 and the homologous recombination protein Rad52 has also been demonstrated (Gómez et al. 2008). However, how these recruiting partners cooperate or compete with each other is unknown.

Recruitment of the NuA4 complex to the sites of DSBs has several outcomes. There is evidence that the recruitment of variant H2A.Z and its subsequent acetylation by KAT5 are an essential early step in the DNA damage response (Gursoy-Yuzugullu, Ayrapetov, and Price 2015; Morillo-huesca et al. 2010; Papamichos-Chronakis et al. 2011; Xu et al. 2012). H2A.Z must be acetylated and then removed so that KAT5 can acetylate H4 (Bird et al. 2002; Clarke et al. 2017; Downs et al. 2004; Doyon et al. 2004; Murr et al. 2005). Acetylation of the damage specific phosophorylated histone variant γ-H2A(X) promotes its turnover (Ikura et al. 2007; Jha, Shibata, and Dutta 2008; Sharma et al. 2010; Soria, Polo, and Almouzni 2012). There is also evidence that NuA4 acetylates the ssDNA binding protein RPA, to regulate resection (Cheng et al. 2018; Kobayashi et al. 2010; Xu et al. 2010). This activity may be important to activate the homologous recombination pathway as opposed to

other types of repair (Jacquet et al. 2016; Renaud, Barascu, and Rosselli 2015).

In fission yeast, Mst1 has multiple activities in chromosome structure, heterochromatin assembly, centromere function, and transcription (Gómez et al. 2008; H. S. Kim et al. 2009; Minoda et al. 2005; Nugent et al. 2010; Xhemalce and Kouzarides 2010). Previously, we showed that a temperature sensitive mutation *mst1*$_{ts}$ (*mst1*Δ *nmt:mst1-L344S*) results in sensitivity to DNA damaging agents even at permissive temperatures (Gómez et al. 2008; Gómez, Espinosa, and Forsburg 2005). Although we showed that *mst1*$_{+}$ affects transcription of a variety of genes, changes in expression do not appear sufficient to account for its DNA damage sensitivity (Nugent et al. 2010). Here, we present evidence that *mst1*$_{+}$ affects DSB repair in fission yeast. We show that Mst1 is recruited to DNA double strand breaks. *mst1-L344S* cells show defects in recruiting downstream factors including Rad52 and RPA. Interestingly, this phenotype is partially rescued by deletion of the end-binding protein pKu70, normally required for NHEJ repair. Our data suggest that Mst1 contributes to efficient resection. Finally, a non-acetylatable H2A.Z mutant (*pht1-4KR*) phenocopies *mst1-L344S*, indicating that H2A.Z may be an important substrate for this effect.

Materials and methods

Strains and Media

Fission yeast cells were grown in YES (yeast extract with supplements) or PMG (pombe minimal glutamate) with appropriate supplements (Sabatinos and Forsburg 2010). Yeast strains used in this research are listed in Table S1 in the supplemental material.

Serial Dilution plating

Yeast cell cultures were grown at 25ºC in YES for two days. Cultures were diluted in YES to equal concentrations. Five-fold serial dilutions of the cultures were then spotted onto YES plates containing different concentrations of drugs. Plates were incubated at 25ºC or 32ºC for the time indicated in each figure legend.

Determination of DSB-induced recombination rates

DSB-induced recombination outcomes were determined using the strain *ade6-M26 int::pUC8/ura4+/MATa/ade6-L469* described in (Fortunato, Osman, and Subramani 1996; Schuchert and Kohli 1988). The *S. cerevisiae* homothallic endonuclease (HO) was expressed on a plasmid from the *nmt1* promoter. Cells were first grown up in PMG (pombe minimal glutamate) liquid media lacking uracil and thiamine (PMG -ura -thia) for two days. Cell cultures were then plated onto PMG -ura -leu +thia agar media for five days at 25ºC. After the five-day incubation, colonies were then streaked onto PMG -leu -thia agar media and incubated at 25ºC for seven days (HO expression induced). Three colonies from each induced-break plate were then selected and serially diluted 1:100 in sterile MilliQ H2O. 100µl of the diluted cultures was plated onto PMG low ade -leu -thia agar media. Agar plates were incubated at 25ºC. After the 14-day incubation, red, white and red/white half

100 sectored colonies were counted and marked. Plates were then replica plated onto PMG -leu -ade -thia and PMG -
101 ade, -ura -thia and allowed to grow for another six days at 25ºC before counting colonies with each phenotype.
102 At least three biological replicates were performed. About 8% are likely "complex" rearrangement, for example
103 colonies that were red/white half sectored on PMG low ade -leu -thia agar media. These colonies arise from
104 recombination intermediates that were not repaired before replication (Fortunato, Osman, and Subramani 1996).

105 **Live-cell imaging and Quantitative Measurements**

106 Live cells imaging was performed as described in (Green, Sabatinos, and Forsburg 2015). Yeast cell
107 cultures were grown at 25ºC in YES overnight. Cells were transferred into PMG + HULAA (Histidine, Uracil,
108 Leucine, Adenine, Arginine) liquid cultures at 25ºC for 16 hours before treating with the indicated drugs for four
109 hours. Cells were collected at OD_{595} 0.3 -0.6, concentrated by centrifuging 1ml at 1500g for 1min and resuspended
110 in 40µl. Concentrated cells were placed on a thin-film pad of 2% agarose in PMG+HULAA on a glass slide. A
111 coverslip was added. Live cells were imaged on DeltaVision Core microscope with softWoRx v4.1 (GE, Issaquah,
112 WA), using a 60X lens, and then deconvolved and projected in softWoRx software. Images were acquired in 13
113 0.2µm z-sections, then deconvolved and Maximum Intensity Projected (softWoRx, default settings). Two
114 separate fields were imaged in each experiment, and 2 to 4 biological replicates were assessed for consistency.
115 Images for publication were contrast adjusted using an equivalent histogram stretch on all samples. Color balance
116 was adjusted, and scale bars were added in Fiji (Schindelin et al. 2012). Significance was calculated using the
117 Mann-Whitney U test.

118 **LacO LacI-mCherry DSB array colocalization with CFP-tagged Rad52**

119 Co-localization was performed as described in (Yu et al. 2013). Cells were cultured at 25ºC in PMG +
120 HULAA (Histidine, Uracil, Leucine, Adenine, Arginine) +Thiamine liquid media to OD_{595} of 0.4-0.6. Cells were
121 then washed twice with PMG +HULAA medium and incubated at 25ºC for 19 hours to induce HO-driven DSB
122 break. Following induction, cells were collected at OD_{595} of 0.3 to 0.6, and were processed and imaged as
123 described above.

124 **Chromatin Immunoprecipitation (ChIP) assay**

125 Chromatin immunoprecipitation (ChIP) was performed as in (Du, Nakamura, and Russell 2006). Cells
126 were grown in EMM+HULA+Thiamine overnight to OD_{595}~0.6. Cells were washed 3 times with EMM+HULA
127 and released in EMM+HULA-Thiamine at 32ºC with shaking. Samples were taken after 14hrs (T=0), 20hrs (T=6),
128 22hrs(T=8), 24hrs (T=10), 26hrs (T=12) and 28hrs (T=14). All samples were fixed with 1% formaldehyde for
129 20min followed by 5 minutes quenching with Glycine. Cells were lysed in standard ChIP buffer and
130 immunoprecipitations were set up using antibodies against GFP (Abcam290), V5(Abcam15828), and Myc
131 (Abcam9132). DNA was column purified using a Qiagen PCR purification kit and multiplex PCR was done as

132 described previously (Du et al 2006). PCR gels were scanned on the BioRad FX scanner and quantified using the
133 Quantity One software.

134 **Western Blots**

135 For the time course experiment, cells were grown at 32$_o$C in YES to OD$_{595}$~0.6 then treated with 40μM
136 camptothecin for 4hrs. Cells were washed three times with YES, then released in YES without drug. Time points
137 were taken at T=0 (before addition of drug), T=4 (after 4hrs of drug treatment), and T=6, 8 (two and four hours
138 after removal of drug). Cells were lysed in 20% TCA. Antibodies against phosphorylated H2A (Abcam 17353)
139 and control PCNA (Santa Cruz-56 PC10) were used. For the Chk1-HA phosphorylation experiment, cells were
140 grown at 32$_o$C in YES to OD$_{595}$~0.6 then treated for 4hrs with 40μM camptothecin, 15mM HU or 0.01%MMS
141 then cells were processed as described above. An anti-HA antibody (12CA5 Abcam16918) was used.

142

143 **Results**

144 **Mst1 is important for double-strand break repair in *S. pombe***

145 Mst1 homologs in mammalian cells (TIP60) and *S. cerevisiae* (*ESA1*) are known to be important for DSB
146 repair (Bird et al. 2002, Sun et al. 2005, Ikura et al. 2007, Tang et al. 2006, rev. Ghobashi and Kamel 2018). We
147 have previously shown that a *S. pombe mst1*$_+$ temperature sensitive allele (*mst1-L344S*) renders cells sensitive to
148 various DNA damaging drugs (Gomez *et al* 2008). Here we expand these studies to further dissect the role of
149 *mst1*$_+$ in DSB repair.

150 Our original *mst1-L344S* construct is expressed from the *nmt1* promoter inserted at the *leu1*$_+$ locus in a
151 deletion background (*mst1*Δ *nmt:mst1-L344S)* Gómez et al. 2008) but more recently, the same allele was been
152 engineered at the native locus under control of the endogenous *mst1*$_+$ promoter (*mst1-L344S*) (Garabedian et al.
153 2012). We tested the sensitivity of both versions to bleomycin, which creates single and double strand DNA
154 breaks (Stubbe and Kozarich 1987; Burger 1998). Both these strains were modestly sensitive to the drug at 25ºC
155 (Figure 1; Gómez et al. 2008), consistent with a requirement for Mst1 in DSB repair. Because the newer *mst1-*
156 *L344S* allele does not generate autofluorescence to the same extent as our original allele, we employed it here for
157 visual assays.

158 We investigated the role of *mst1*$_+$ in repair of a single DSB break. We first utilized a strain that uses the
159 homothallic switching endonuclease (HO) to induce a single double strand break between two non-tandem repeats
160 as originally described by (Schuchert and Kohli 1988) and modified by (Osman, Adriance, and McCready 2000)
161 (Figure 2A). In this strain, a functional *ura4*$_+$ gene is flanked by two full length non-functional *ade6* alleles, each
162 containing a different point mutation. The HO endonuclease makes a DSB at *MATa* site adjacent to *ura4*$_+$. The
163 repair outcomes can be determined by selecting Ade$_+$ cells and screening for Ura$_+$ (Ahn, Osman, and Whitby
164 2005; Fortunato, Osman, and Subramani 1996; Osman, Adriance, and McCready 2000; Osman, Fortunato, and

165 Subramani 1996). Uracil auxotrophic colonies ("deletion type", whether Ade+ or Ade-) result from deletion and
166 rearrangement, in which cells repaired the lesion by Single Strand Annealing (SSA), Non-Homologous End-
167 Joining (NHEJ), or more complex rearrangements. In contrast, Ade+ colonies that retain Ura+ ("conversion type")
168 are presumed to derive from gene conversion via homologous recombination.

169 Following induction of the DSB, we observed that the survival of *mst1-L344S* was much lower than the
170 survival in wild-type cells (Figure 2B), consistent with a repair defect. In wild-type cells, about 55.64% of
171 colonies are deletion type (Ade+/Ade- Ura-) while 36.70% of colonies were conversion type (Ade+ Ura+) (Figure
172 3C). In the surviving *mst1-L344S* cells, we observed a significantly higher percentage of colonies showing
173 deletion-type repair (75.3%) than in wild type (Figure 2C). These data suggest that wild type *mst1*+ biases repair
174 towards conversion-type, error-free recombination.

175 To examine whether Mst1 physically localizes to DSB breaks as has been reported for *Hs*TIP60 and
176 *Sc*Esa1 (Downs and Jackson 2004; Sun et al. 2009), we employed a strain previously engineered to test
177 recruitment of proteins by ChIP to one single double strand break (Figure 2D) (Du, Nakamura, and Russell 2006).
178 This assay can monitor both temporal and spatial recruitment of proteins to a single DSB. Mst1-V5 appears to
179 arrive at the break before Mre11-myc and Rad52-YFP. By 12h post-induction, Mre11 becomes concentrated at
180 the break (compare 0.2Kb oh with 12h). We also find that Mst1 and Rad52 spread away from the break while
181 Mre11 remains localized.

182

183 **Mst1 contributes to recruitment of repair factors to DSBs**

184 We examined the recruitment of homologous recombination proteins in *mst1-L344S* cells using a visual
185 screen. First, we looked at the localization of Rad52 and RPA proteins in response to phleomycin (an analog of
186 bleomycin; Belenguer et al. 1995) using live-cell imaging (Figure 3A, Supplementary Figure S1). We observed
187 that phleomycin treatment generates a lower percentage of *mst1-L344S* cells with repair foci compared to wild-
188 type. We also imaged cells with GFP-tagged Rad54, a recombination protein that is downstream of Rad52 (Figure
189 3B; Onaka et al. 2016). Similar to RPA and Rad52, fewer *mst1-L344S* cells showed Rad54 foci (Figure 3B).
190 These observations suggest that Mst1 is required for the normal recruitment of downstream HR factors.

191 Next, we examined the recruitment of Rad52 at a specific DSB site. We utilized a strain that contains a
192 mCherry-LacI marked HO-induced DSB and CFP-tagged Rad52 (Yu et al. 2013). We imaged both wild-type and
193 *mst1-L344S* cells over a four-hour period. In wild-type cells, we observed that 75% of total Rad52 foci co-localize
194 with mCherry-DSB foci until 100 minutes (Figure 3C top). After 100 minutes, the percentage of colocalization
195 dropped in wild type, because the mCherry-LacI signal disappears (Figure 3C bottom and Figure 3D). This loss
196 of mCherry-lacI presumably reflects resection at DSBs that eliminates the LacO target (Leland et al. 2018; Yu et

197 al. 2013). Consistent with prior reports, we observed that the mCherry-DSB foci dropped to 25% by the end of
198 four-hour time-course (Figure 3D, Yu et al. 2013). In contrast, in *mst1-L344S* cells, fewer than 40% of total Rad52
199 foci colocalize with mCherry-DSB foci across the four-hour time-course (Figure 3C top). Strikingly, however,
200 over 90% of mCherry-DSB signal remained even at the end of the time-course (Figure 3C bottom and Figure
201 3D). This suggests that in the absence of functional Mst1, resection is inhibited.

202 **Processing of DSBs and a role for Ku**

203 The heterodimeric Ku complex is very abundant and binds rapidly and immediately to DSBs (Fell and
204 Schild-Poulter 2015; Shibata, Jeggo, and Löbrich 2018). Ku inhibits initial resection driven by MRN, while MRN
205 removes Ku to promote proper resection and facilitate homologous recombination (HR) (Langerak et al. 2011;
206 Myler et al. 2017; Shao et al. 2012; Shibata, Jeggo, and Löbrich 2018; Tomita et al. 2003). Unexpectedly, we
207 found that *pku70*Δ partially rescues the bleomycin sensitivity of *mst1-L344S* (Figure 1).

208 We wondered whether pKu70 also affects the recruitment of repair proteins in *mst1-L344S*. Therefore, we
209 imaged fluorescently tagged RPA under phleomycin treatment and observed that the percentage of cells with
210 RPA foci in *pku70*Δ and *pku70*Δ *mst1-L344S* is higher than in *mst1-L344S*, although the percentage is still
211 significantly lower than that in wild-type cells (Figure 3A). We also observed a higher fraction of *pku70*Δ *mst1-*
212 *L344S* cells with Rad52 foci in phleomycin treatment than either *mst1-L344S* or *pku70*Δ single mutants (Figure
213 3A). The percentage of cells with Rad54 foci increases in *mst1-L344S pku70*Δ compared to *mst1-L344S* and is
214 similar to that in wild-type (Figure 3B).

215 Next, we used the mCherry-LacI marked HO-induced DSB system to examine the apparent resection of
216 DSB in *pku70*Δ mutants (Figure 3D). We find that *pku70*Δ single mutant cells do show a reduction in mCherry-
217 DSB foci over time, but this effect is far more modest than that in wild-type. At the end of the time-course, just
218 under 70% of the *pku70*Δ cells still contain mCherry-DSB foci. We observed a similar phenotype in *pku70*Δ *mst1-*
219 *L344S* cells, indicating that the loss of *pku70* is epistatic to the *mst1* phenotype (Figure 3D).

220 Long range resection is initiated by MRN and extended by the exonuclease Exo1, as well as other proteins
221 (Langerak et al. 2011; Zhu et al. 2008). We observed that mCherry-LacI marked DSBs do not disappear over the
222 time-course in *exo1*Δ, in contrast to wild-type (Figure 3D), and consistent with a failure in resection. We observed
223 that *exo1*Δ*, mst1-L344S,* and the double mutant *exo1*Δ *mst1-L344S* all show a similar persistence of the mCherry
224 signal. Additionally, *exo1*Δ *mst1-L344S* has similar sensitivity to bleomycin as the *mst1-L344S* single mutant and
225 this sensitivity is rescued by *pku70*Δ (Figure 1). These data suggest that *mst1*+ and *exo1*+ are in the same epistatic
226 pathway (Figure 1).

227 Finally, we observed that percentage of cells with repair foci in *mst1-L344S pku70*Δ double mutant is
228 higher even in untreated cells, compared to wild-type or *mst1-L344S* single mutants (Figure 3). This suggests that
229 there is an intrinsic genome instability in the double mutant, although cell growth and cell length at septation were
230 not significantly affected (Figure 1; Supplementary Figure S2).

231 **Is H2A.Z a target of Mst1 to regulate DSB repair**?

232 It is known in other organisms that the presence and turnover of the histone variant H2A.Z (*S. pombe*
233 Pht1), a KAT5 substrate, is important for the proper repair of DSBs by regulating resection (Gursoy-Yuzugullu,
234 Ayrapetov, and Price 2015; Y. Jiang et al. 2015; Xu et al. 2012). In human cells, H2A.Z depletion leads to higher
235 ssDNA accumulation and lower DSB recovery from HR (Y. Jiang et al. 2015; Xu et al. 2012). Failure to remove
236 H2A.Z at DSBs in human cells leads to higher RPA binding and higher recovery from HR (Gursoy-Yuzugullu,
237 Ayrapetov, and Price 2015). In fission yeast, H2A.Z is a known substrate of Mst1, and a mutant *pht1-4KR* that
238 disrupts the Mst1 acetylation sites causes genome instability and anaphase defects (H. S. Kim et al. 2009). To
239 investigate the role of H2A.Z acetylation in repair, we compared the phenotype of *pht1-4KR* to *mst1-L344S.* We
240 observed significant reduction in RPA and Rad52 foci in *pht1-4KR* at 25ºC similar to that observed with *mst1-*
241 *L344S* cells (Figure 3A). However, the sensitivity to bleomycin we observe in *pht1-4KR* is not rescued by *pku70*Δ
242 (Figure 1).

243 We also compared the phenotypes of *pht1*Δ and *pht1-4KR* cells. *pht1*Δ showed fewer cells with RPA foci
244 compared to wild type under phleomycin treatment (Figure 3A). Rad52 foci were also reduced in *pht1*Δ compared
245 to wild type under phleomycin treatment (Figure 3A). However, the effect of *pht1-4KR* cells was more dramatic
246 than *pht1*Δ*,* and much closer to the observations in *mst1-L344S.* (Figure 3A). We also examined the mCherry-
247 DSB reporter system to identify resection. As with *mst1-L344S* and *exo1*Δ, *pht1-4KR* cells showed a persistent
248 mCherry-DSB signal, consistent with a failure to resect (Figure 3D).

249 **The damage checkpoint is normal in *mst1-L344S***

250 Previously, we showed that the temperature-sensitive allele *mst1*Δ *leu1*$_+$*::nmt-mst1-L344S* is sensitive to
251 S-phase specific genotoxins including methyl methanesulfonate (MMS), which causes alkylation damage that
252 inhibits replication, and camptothecin (CPT), a topoisomerase-I inhibitor that causes lesions during S-phase
253 (Frampton et al. 2006; Fung et al. 2002; Morishita et al. 2003; Wan, Capasso, and Walworth 1999). In contrast to
254 our observations with phleomycin, we observed that the percentage of cells with RPA and Rad52 foci was higher
255 in *mst1-L344S* cells treated with these S-phase specific genotoxins than that in wild-type (Figure 4A). This is
256 consistent with different repair pathways being activated by these S–phase specific lesions.

257 We examined genetic interactions between *mst1-L344S* and mutants that affect checkpoint and repair

258 responses under treatment with a variety of S-phase specific genome stressors (Supplementary Figure S3). A
259 modest growth defect in untreated cells was observed for the double mutant *mst1-L344S rad3*Δ but not for others.
260 In cells treated with UV or MMS at 25ºC, we observed a striking negative interaction between *mst1-L344S* and
261 damage checkpoint mutants *chk1*Δ or *crb2*Δ at 25ºC, suggesting a requirement for an active damage checkpoint
262 response under these treatments. We treated cells with MMS, CPT or HU and performed western blots against
263 HA tagged Chk1. In wild-type, Chk1 is phosphorylated in cells treated with four-hour CPT or MMS, but not in
264 untreated cells or cells treated with HU (Figure 4B;Walworth and Bernards 1996). We observed a similar
265 phosphorylation pattern in *mst1-L344S* mutant (Figure 4B). H2A phosphorylation, one of the first sensors of DNA
266 damage and double strand breaks, was also present in *mst1-L344S* cells after 4-hour CPT treatment as in wild-
267 type cells and diminished after removing drugs from cell culture (Figure 4C). Mst1 is not required for checkpoint
268 activation in response to S-phase specific lesions but depends on that response for viability.

269

270 **Discussion**

271 The MYST protein Mst1 (hTIP60; ScEsa1; KAT5) is the catalytic subunit of the NuA4 histone
272 acetyltransferase complex, and makes pleiotropic contributions to genome stability (rev. in (Lafon et al. 2007;
273 Pillus 2008)). Multiple studies indicate that hTIP60 and ScEsa1 contribute to DSB repair through acetylation (rev.
274 in (Ghobashi and Kamel 2018)), and show that the acetyltransferase binds near DSB regions (Cheng et al. 2018;
275 Li and Wang 2017; Sun et al. 2009; Xu et al. 2010). The budding yeast ScEsa1 acetylates ssDNA binding protein
276 RPA at DSBs (Xue; Cheng et al. 2018) and in mammalian cells, Tip60 promotes HR localization of recombination
277 protein Rad51 (Murr et al. 2005).

278 Previously we showed that Mst1 is *S. pombe* is essential for viability and we demonstrated the sensitivity
279 of *mst1*Δ *nmt:mst1-L344S* to a number of genotoxins (Gómez et al. 2008; Gómez, Espinosa, and Forsburg 2005).
280 However, the autofluorescence of this particular construct precluded analysis of repair markers *in vivo.* A different
281 version of the same *mst1-L344S* allele integrated at the endogenous locus has reduced viability at the semi-
282 permissive 32ºC compared to *mst1*Δ *nmt:mst1-L344S* (Garabedian et al. 2012), but showed a similar range of
283 sensitivities (Figure 1) and no autofluorescence. In this paper, we have further investigated Mst1's role in DNA
284 damage response and its function in DSB repair using this version of the conditional allele.
285 We confirmed that Mst1 in *S. pombe* is important for DSB repair because both temperature sensitive
286 alleles are sensitive to a DSB-inducing environment including treatment phleomycin or bleomycin, and
287 constitutive HO-nuclease expression (Figure 1, 2B and 3). Additionally, our data indicate that Mst1 directly
288 localizes to DSBs (Figure 2D). We observed that that even under permissive growth conditions, *mst1-L344S* shifts
289 the balance of repair away from HR towards SSA or NHEJ (Figure 2C). We also observed a lower percentage of

290 *mst1-L344S* cells compared to wild type show visible foci of HR proteins, including RPA, Rad52 and Rad54.
291 These observations suggest that Mst1 facilitates homologous recombination to repair DSBs, and in its absence,
292 HR is impaired (Figure 5).

293 There are conflicting data as to whether Kat5/NuA4 influences non-homologous end joining (NHEJ),
294 which is typically the alternative pathway for repair if HR is inhibited (Chang et al. 2017). In budding yeast,
295 ScEsa1 has been reported to be essential for NHEJ at DSBs (Bird et al. 2002). However, studies in mammalian
296 cells suggest hTIP60 instead inhibits NHEJ by acetylating H2A and H4; this reduces loading of 53BP1 protein
297 that promotes NHEJ (Jacquet et al. 2016; Renaud, Barascu, and Rosselli 2015; J. Tang et al. 2013). Consistent
298 with this, in, budding yeast deletion of the 53BP1 orthologue Sc*rad9* increases resection efficiency (Bonetti et al.
299 2015) and similarly, fission yeast *crb2*Δ mutants have increased resection (Leland et al. 2018). We did not
300 specifically examine efficiency of NHEJ, but our data suggest that Mst1 affects homologous recombination, and
301 that long-range resection is defective in a *mst1* mutant (Figure 3 and Figure 5).

302 To monitor resection, we used a visual assay in which a lacO array marked by lacI-mCherry is adjacent
303 to an induced double strand break. Previous studies have shown that loss of the lacO array adjacent to a break
304 correlates with resection (Leland et al. 2018; Yu et al. 2013). Indeed, we find that the mCherry signal declines
305 over time in a wild type in the presence of the induced break, but not in an *exo1*Δ mutant that lacks the long-range
306 exonuclease. We observe that *mst1-L344S* resembles *exo1*Δ in this assay. The data from this, as well as sensitivity
307 to DSB-inducing drugs, suggest that *mst1* and *exo1* are in a common epistasis group (Figure 5).

308 The end-binding protein complex Ku inhibits resection and thus, homologous recombination (rev. in
309 Shibata, Jeggo, and Löbrich 2018). Its activity is coordinated with the Mre11-Rad50-Nbs1 (MRN) complex
310 associated with early steps in resection (rev. in Shibata, Jeggo, and Löbrich 2018; Syed and Tainer 2018). While
311 Ku inhibits resection driven by MRN, MRN removes Ku to facilitate homologous recombination (HR) over NHEJ
312 (Langerak and Russell 2011; Myler et al. 2017; Shao et al. 2012; Shibata, Jeggo, and Löbrich 2018). Previous
313 work has shown that *pku70*Δ rescues resection in the absence of the MRN complex (Langerak et al. 2011;
314 Teixeira-Silva et al. 2017; Tomita et al. 2003). Consistent with this, we found that deletion of pKu70 partially
315 rescues *mst1* and *mst1 exo1*Δ sensitivity to DSB-inducing agents, and partly restores recruitment of HR proteins.
316 The *pku70*Δ *mst1-L344S* cells show similar percentage of RPA foci as in *pku70*Δ single mutant in phleomycin,
317 but a higher percentage of cells with Rad52 than either *pku70*Δ or *mst1-L344S* alone. We also observe an
318 intermediate effect of pKu70 on resection in our visual assay. These observations suggest that Mst1 activity is
319 required to antagonize a Ku-associated function that inhibits HR (Figure 5).

320 Multiple studies show the presence and the turnover of the histone variant H2A.Z (SpPht1) is required
321 for DSB repair (Gursoy-Yuzugullu, Ayrapetov, and Price 2015; Y. Jiang et al. 2015; Kalocsay, Hiller, and Jentsch
322 2009; Xu et al. 2012). In mammalian cells, the absence of H2A.Z leads to more ssDNA accumulation and reduced

323 pKu70 localization (Gursoy-Yuzugullu, Ayrapetov, and Price 2015; Xu et al. 2012). We observed fewer cells
324 with RPA foci in *pht1*Δ. Indeed, the loss of resection in *mst1* mutants can be partially rescued by deletion of
325 *pku70*, similar to the rescue of MRN mutants by Ku. Again, this places *mst1* genetically in a pathway leading to
326 resection (Figure 5).

327 Exchange of H2A.Z is required for H4 acetylation by hTip60, which creates open chromatin (Downs et
328 al. 2004; Gursoy-Yuzugullu, Ayrapetov, and Price 2015; Murr et al. 2006; Sun et al. 2009; Xu et al. 2010, 2012).
329 Several acetyltransferases have been implicated in H2A.Z acetylation including Kat5 (Mst1) and Kat2A (Gcn5)
330 (Babiarz, Halley, and Rine 2006; Keogh et al. 2006; H. S. Kim et al. 2009; Kusch et al. 2004; Millar et al. 2006;
331 Semer et al. 2019; Zlatanova and Thakar 2008). In mammalian cells, the deposition of H2A.Z precedes its
332 acetylation (Xu et al. 2012), while in Drosophila, the acetylation of H2A.Z homolog H2Av stimulates its removal
333 after DNA damage (Kusch et al. 2004). Blocking Tip60 prevents both H2A.Z exchange and H4 acetylation
334 (Morillo-huesca et al. 2010; Papamichos-Chronakis et al. 2011; Shastri et al. 2018; Xu et al. 2012).

335 To investigate whether H2A.Z acetylation by Mst1 influences repair, we used a non-acetylable mutant of
336 H2A.Z, *pht1-4KR*. This mutation has previously been shown to disrupt Mst1 acetylation sites and leads to
337 chromosome segregation errors (H. S. Kim et al. 2009). We saw a similar percentage of *pht1-4KR* cells with RPA
338 and Rad52 foci as that in *mst1-L344S* cells, both significantly lower than that in wild type. Additionally, mCherry-
339 DSB foci in *pht1-4KR* did not disappear across the time-course, and the percentage of mCherry-DSB persistence
340 was similar to that in *mst1-L344S* (Figure 3D). This suggests that *pht1-4KR* and *mst1-344S* are in a common
341 epistasis group. We propose that acetylation of H2A.Z by Mst1 facilitates the subsequent removal of H2A.Z at
342 DSBs. We suggest that *pht1-4KR* once inserted cannot be efficiently removed, and prevents H4 acetylation and
343 chromatin decompaction essentially locking the chromatin in a form refractory to long range resection. Consistent
344 with this model, the sensitivity of *pht1-4KR* to DSBs is more severe than that of *pht1*Δ, suggesting that an
345 immobile H2A.Z is more damaging than no H2A.Z at all. Since *pht1-4KR* sensitivity to bleomycin is not rescued
346 by *pku70*Δ (Figure 1), we propose that H2A.Z binds to DSBs after pKu70 is removed, and therefore removing
347 pKu70 cannot rescue the immobilization of H2A.Z.

348 Finally, we show that the temperature sensitive allele *mst1*Δ *leu1*$_{+}$*::nmt:mst1-L344S* is sensitive to S phase
349 specific genotoxins including methyl methanesulfonate (MMS) and camptothecin (CPT) (Gómez et al. 2008).
350 Studies in *S. cerevisiae* also showed Esa1's importance to MMS-induced damage repair (Bird et al. 2002; Renaud-
351 Young et al. 2015). This is consistent with a recent study showing that Mst1 in *S. pombe* is important for CPT-
352 induced damage repair (Noguchi et al. 2019).

353 Compromised DNA damage repair could be the result of defective damage checkpoint activation. In
354 mammalian cells, TIP60 is known to activate signaling pathway by acetylating ATM and p53 (Sun et al. 2005;

355 Sykes et al. 2006; Y. Tang et al. 2006). However, we find that the temperature sensitive allele *mst1*Δ *mst1-L344S*
356 does not affect activation DNA damage checkpoint Chk1 or phosphorylation of H2A(X).
357 Taken together, our data suggest that SpMst1contributes to repair of a variety of DNA lesions. As in other
358 organisms, our data show that Mst1 acetyltransferase has a particular role in double strand break repair, where it
359 facilitates homologous recombination by promoting long range resection and antagonizing NHEJ-promoting
360 factors such as Ku (Figure 5). Our data suggest that this depends on acetylation of H2A.Z. The conservation of
361 function of this acetyltransferase across eukaryotes indicates the fundamental nature of chromatin modification
362 in DNA repair transactions.
363
364 Acknowledgement
365 We would like to thank Li-Lin Du, Michael Keogh, Takuro Nakagawa, Eishi Noguchi, Mathew
366 O'Connell, and Simon Whitehall for strains. We thank Ji-Ping Yuan and Amanda Jensen for assistance and
367 technical support. We are grateful to current members of the Forsburg lab for many helpful comments and
368 discussions throughout the course of the study. This work was supported by
369

370 **References**

371 Ahn, Jong Sook, Fekret Osman, and Matthew C. Whitby. 2005. "Replication Fork Blockage by RTS1 at an
372 Ectopic Site Promotes Recombination in Fission Yeast." *EMBO Journal* 24(11): 2011–23.

373 Allard, Stéphane et al. 1999. "The NuA4 Transcription Activation/Histone H4 Acetyltransferase Complex
374 Contains the Essential Esa1 Protein as the Catalytic Subunit and the Essential ATM-Related Cofactor
375 Tra1p." *Biochemistry and Cell Biology* 77(4): 5108–19.
376 http://www.nrcresearchpress.com/doi/10.1139/o99-903.

377 Avvakumov, N.;, and J. Côté. 2007. "The MYST Family of Histone Acetyltransferases and Their Intimate
378 Links to Cancer." *Oncogene* 26(37): 5395–5407.

379 Ayrapetov, M. K. et al. 2014. "DNA Double-Strand Breaks Promote Methylation of Histone H3 on Lysine 9
380 and Transient Formation of Repressive Chromatin." *Proceedings of the National Academy of Sciences*
381 111(25): 9169–74. http://www.pnas.org/cgi/doi/10.1073/pnas.1403565111.

382 Babiarz, Joshua E., Jeffrey E. Halley, and Jasper Rine. 2006. "Telomeric Heterochromatin Boundaries Require
383 NuA4-Dependent Acetylation of Histone Variant H2A.Z in Saccharomyces Cerevisiae." *Genes and*
384 *Development*.

385 Bakkenist, Christopher J., and Michael B. Kastan. 2015. "Chromatin Perturbations during the DNA Damage
386 Response in Higher Eukaryotes." *DNA Repair* 36: 8–12.

387 Belenguer, P., M.-L. Oustrin, G. Tiraby, and B. Ducommun. 1995. "Effects of Phleomycin-Induced DNA
388 Damage on the Fission Yeast Schizosaccharomyces Pombe Cell Cycle." *Yeast* 11(3): 225–31.

389 Bird, A W; et al. 2002. "Acetylation of Histone H4 by Esa1 Is Required for DNA Double-Strand Break Repair."
390 *Nature* 419(September): 411–15. http://www.ncbi.nlm.nih.gov/pubmed/12353039.

391 Bonetti, Diego et al. 2015. " Escape of Sgs1 from Rad9 Inhibition Reduces the Requirement for Sae2 and
392 Functional MRX in DNA End Resection ." *EMBO reports* 16(3): 351–61.

393 Burger, Richard M. 1998. "Cleavage of Nucleic Acids by Bleomycin." 2665(96): 16–19.

394 Chang, Howard H.Y., Nicholas R. Pannunzio, Noritaka Adachi, and Michael R. Lieber. 2017. "Non-
395 Homologous DNA End Joining and Alternative Pathways to Double-Strand Break Repair." *Nature*
396 *Reviews Molecular Cell Biology* 18(8): 495–506. http://dx.doi.org/10.1038/nrm.2017.48.

397 Cheng, Xue; et al. 2018. "Phospho-Dependent Recruitment of NuA4 by MRX at DNA Breaks Regulates RPA
398 Dynamics during Resection." *Proceedings of the National Academy of Sciences of the United States of*
399 *America* 6(Suppl 1): P93. http://www.pnas.org/content/pnas/early/2018/09/13/1806513115.full.pdf.

400 Cheng, Xue et al. 2018. "Phospho-Dependent Recruitment of the Yeast NuA4 Acetyltransferase Complex by
401 MRX at DNA Breaks Regulates RPA Dynamics during Resection." *Proceedings of the National Academy*
402 *of Sciences of the United States of America* 115(40): 10028–33.

403 Clarke, Thomas L.; et al. 2017. "PRMT5-Dependent Methylation of the TIP60 Coactivator RUVBL1 Is a Key
404 Regulator of Homologous Recombination." *Molecular Cell* 65(5): 900–916.
405 http://dx.doi.org/10.1016/j.molcel.2017.01.019.
406 Downs, Jessica A. et al. 2004. "Binding of Chromatin-Modifying Activities to Phosphorylated Histone H2A at
407 DNA Damage Sites." *Molecular Cell* 16(6): 979–90.
408 Downs, Jessica A., and Stephen P. Jackson. 2004. "A Means to a DNA End: The Many Roles of Ku." *Nature*
409 *Reviews Molecular Cell Biology* 5(5): 367–78.
410 Doyon, Yannick et al. 2004. "Structural and Functional Conservation of the NuA4 Histone Acetyltransferase
411 Complex from Yeast to Humans." *Molecular and cellular biology* 24(5): 1884–96.
412 http://www.pubmedcentral.nih.gov/articlerender.fcgi?artid=350560&tool=pmcentrez&rendertype=abstract
413 .
414 Doyon, Yannick, and Jacques Côté. 2004. "The Highly Conserved and Multifunctional NuA4 HAT Complex."
415 *2* 14(2): 147–54.
416 Du, Li Lin, Toru M. Nakamura, and Paul Russell. 2006. "Histone Modification-Dependent and -Independent
417 Pathways for Recruitment of Checkpoint Protein Crb2 to Double-Strand Breaks." *Genes and Development*
418 20(12): 1583–96.
419 Fell, Victoria L., and Caroline Schild-Poulter. 2015. "The Ku Heterodimer: Function in DNA Repair and
420 Beyond." *Mutation Research - Reviews in Mutation Research* 763: 15–29.
421 http://dx.doi.org/10.1016/j.mrrev.2014.06.002.
422 Fortunato, Elizabeth A., Fekret Osman, and Suresh Subramani. 1996. "Analysis of Spontaneous and Double-
423 Strand Break-Induced Recombination in Rad Mutants of S. Pombe." *Mutation Research - DNA Repair*
424 364(3): 147–60.
425 Frampton, Jonathan et al. 2006. "Postreplication Repair and PCNA Modification in Schizosaccharomyces
426 Pombe Jonathan." *Molecular Biology of the Cell* 17(April): 2976–85.
427 Fung, A. D., J. Ou, S. Bueler, and G. W. Brown. 2002. "A Conserved Domain of Schizosaccharomyces Pombe
428 Dfp1+ Is Uniquely Required for Chromosome Stability Following Alkylation Damage during S Phase."
429 *Molecular and Cellular Biology* 22(13): 4477–90.
430 Galarneau, Luc et al. 2000. "Multiple Links between the NuA4 Histone Acetyltransferase Complex and
431 Epigenetic Control of Transcription." *Molecular Cell*.
432 Garabedian, Mikael V. et al. 2012. "The Double-Bromodomain Proteins Bdf1 and Bdf2 Modulate Chromatin
433 Structure to Regulate S-Phase Stress Response in Schizosaccharomyces Pombe." *Genetics* 190(2): 487–
434 500.
435 Ghobashi, Ahmed H, and Maher A Kamel. 2018. "Tip60 : Updates." 2: 161–68.

436 Gómez, Eliana B., Rebecca L. Nugent, Sebastián Laria, and Susan L. Forsburg. 2008. "Schizosaccharomyces
437 Pombe Histone Acetyltransferase Mst1 (KAT5) Is an Essential Protein Required for Damage Response
438 and Chromosome Segregation." *Genetics* 179(2): 757–71.
439 Gómez, Eliana B, Joaquín M Espinosa, and Susan L Forsburg. 2005. "Schizosaccharomyces Pombe Mst2+
440 Encodes a MYST Family Histone Acetyltransferase That Negatively Regulates Telomere Silencing."
441 *Molecular and cellular biology* 25(20): 8887–8903.
442 Green, Marc D.;, Sarah A.; Sabatinos, and Susan L.; Forsburg. 2015. "Microscopy Techniques to Examine
443 DNA Replication in Fission Yeast." *Methods Mol Biol* 1300: 13–41.
444 Gursoy-Yuzugullu, Ozge;, Marina K.; Ayrapetov, and Brendan D.; Price. 2015. "Histone Chaperone Anp32e
445 Removes H2A.Z from DNA Double-Strand Breaks and Promotes Nucleosome Reorganization and DNA
446 Repair." *Proceedings of the National Academy of Sciences* 112(24): 7507–12.
447 http://www.pnas.org/lookup/doi/10.1073/pnas.1504868112.
448 Ikura, T. et al. 2007. "DNA Damage-Dependent Acetylation and Ubiquitination of H2AX Enhances Chromatin
449 Dynamics." *Molecular and Cellular Biology* 27(20): 7028–40.
450 http://mcb.asm.org/cgi/doi/10.1128/MCB.00579-07.
451 Jacquet, Karine et al. 2016. "The TIP60 Complex Regulates Bivalent Chromatin Recognition by 53BP1 through
452 Direct H4K20me Binding and H2AK15 Acetylation." *Molecular Cell* 62(3): 409–21.
453 Jha, S., E. Shibata, and A. Dutta. 2008. "Human Rvb1/Tip49 Is Required for the Histone Acetyltransferase
454 Activity of Tip60/NuA4 and for the Downregulation of Phosphorylation on H2AX after DNA Damage."
455 *Molecular and Cellular Biology* 28(8): 2690–2700. http://mcb.asm.org/cgi/doi/10.1128/MCB.01983-07.
456 Jiang, Xiaofeng et al. 2006. "The FATC Domains of PIKK Proteins Are Functionally Equivalent and Participate
457 in the Tip60-Dependent Activation of DNA-PKcs and ATM." *Journal of Biological Chemistry* 281(23):
458 15741–46.
459 Jiang, Yuhui et al. 2015. "Local Generation of Fumarate Promotes DNA Repair through Inhibition of Histone
460 H3 Demethylation." *Nature Cell Biology* 17(9): 1158–68.
461 Judes, Gaëlle et al. 2015. "A Bivalent Role of TIP60 Histone Acetyl Transferase in Human Cancer."
462 *Epigenomics*.
463 Kalocsay, Marian, Natalie Jasmin Hiller, and Stefan Jentsch. 2009. "Chromosome-Wide Rad51 Spreading and
464 SUMO-H2A.Z-Dependent Chromosome Fixation in Response to a Persistent DNA Double-Strand Break."
465 *Molecular Cell* 33(3): 335–43. http://dx.doi.org/10.1016/j.molcel.2009.01.016.
466 Keogh, Michael-christopher; et al. 2006. "The Saccharomyces Cerevisiae Histone H2A Variant Htz1 Is
467 Acetylated by NuA4 The Saccharomyces Cerevisiae Histone H2A Variant Htz1 Is Acetylated by NuA4."
468 *Genes & development* 20(6): 660–65.

469 Kim, Hyun Soo; et al. 2009. "An Acetylated Form of Histone H2A.Z Regulates Chromosome Architecture in
470 Schizosaccharomyces Pombe." *Nature Structural and Molecular Biology* 16(12): 1286–93.
471 http://dx.doi.org/10.1038/nsmb.1688.
472 Kim, M.-Y. et al. 2007. "Tip60 Histone Acetyltransferase Acts as a Negative Regulator of Notch1 Signaling by
473 Means of Acetylation." *Molecular and Cellular Biology*.
474 Kimura, Akatsuki;, and Masami Horikoshi. 1998. "Tip60 Acetylates Six Lysines of a Specific Class in Core
475 Histones in Vitro." *Genes to Cells* 3(12): 789–800.
476 Kobayashi, Junya et al. 2010. "Bisbenzamidine Derivative, Pentamidine Represses DNA Damage Response
477 through Inhibition of Histone H2A Acetylation." *Molecular Cancer* 9: 1–11.
478 Kobor, Michael S et al. 2004. "A Protein Complex Containing the Conserved Swi2/Snf2-Related ATPase
479 Swr1p Deposits Histone Variant H2A.Z into Euchromatin." *PLoS biology* 2(5): 4.
480 http://www.pubmedcentral.nih.gov/articlerender.fcgi?artid=374244&tool=pmcentrez&rendertype=abstract
481 .
482 Krogan, Nevan J.; et al. 2004. "Regulation of Chromosome Stability by the Histone H2A Variant Htz1, the
483 Swr1 Chromatin Remodeling Complex, and the Histone Acetyltransferase NuA4." *Proceedings of the*
484 *National Academy of Sciences* 101(37): 13513–18.
485 Kusch, Thomas et al. 2004. "Acetylation by Tip60 Is Required for Selective Histone Variant Exchange at DNA
486 Lesions." *Science* 306(5704): 2084–87.
487 De La Cruz, Xavier, Sergio Lois, Sara Sánchez-Molina, and Marian A. Martínez-Balbás. 2005. "Do Protein
488 Motifs Read the Histone Code?" *BioEssays*.
489 Lafon, A. et al. 2007. "MYST Opportunities for Growth Control: Yeast Genes Illuminate Human Cancer Gene
490 Functions." *Oncogene* 26(37): 5373–84.
491 Langerak, Petra, Eva Mejia-Ramirez, Oliver Limbo, and Paul Russell. 2011. "Release of Ku and MRN from
492 DNA Ends by Mre11 Nuclease Activity and Ctp1 Is Required for Homologous Recombination Repair of
493 Double-Strand Breaks." *PLoS Genetics* 7(9).
494 Langerak, Petra, and Paul Russell. 2011. "Regulatory Networks Integrating Cell Cycle Control with DNA
495 Damage Checkpoints and Double-Strand Break Repair." *Philosophical Transactions of the Royal Society*
496 *B: Biological Sciences* 366(1584): 3562–71.
497 Leduc, C. et al. 2006. "P14ARF Promotes RB Accumulation through Inhibition of Its Tip60-Dependent
498 Acetylation." *Oncogene*.
499 Leland, Bryan A. et al. 2018. "Rev7 and 53BP1/CRB2 Prevent RecQ Helicase-Dependent Hyper-Resection of
500 DNA Double-Strand Breaks." *eLife* 7: 1–14.
501 Li, Lin, and Yinsheng Wang. 2017. "Cross-Talk between the H3K36me3 and H4K16ac Histone Epigenetic

502 Marks in DNA Double-Strand Break Repair." *Journal of Biological Chemistry* 292(28): 11951–59.
503 Millar, Catherine B.;, Feng; Xu, Kangling; Zhang, and Michael Grunstein. 2006. "Acetylation of H2AZ Lys 14
504 Is Associated with Genome-Wide Gene Activity in Yeast." *Genes and Development* 20(6): 711–22.
505 Miller, Kyle M., and Stephen P. Jackson. 2012. "Histone Marks: Repairing DNA Breaks within the Context of
506 Chromatin." *Biochemical Society Transactions* 40(2): 370–76.
507 Minoda, Aki, Shigeaki Saitoh, Kohta Takahashi, and Takashi Toda. 2005. "BAF53/Arp4 Homolog Alp5 in
508 Fission Yeast Is Required for Histone H4 Acetylation, Kinetochore-Spindle Attachment, and Gene
509 Silencing at Centromere." *Molecular biology of the cell* 16(1): 316–27.
510 Morillo-huesca, Macarena;, Marta; Clemente-ruiz, Eloisa; Andujar, and Félix Prado. 2010. "The SWR1 Histone
511 Replacement Complex Causes Genetic Instability and Genome-Wide Transcription Misregulation in the
512 Absence of H2A . Z." *PLoS ONE* 5(8).
513 Morishita, T., Y. Tsutsui, H. Iwasaki, and H. Shinagawa. 2003. "The Schizosaccharomyces Pombe Rad60 Gene
514 Is Essential for Repairing Double-Strand DNA Breaks Spontaneously Occurring during Replication and
515 Induced by DNA-Damaging Agents." *Molecular and Cellular Biology* 23(9): 3373–3373.
516 Murr, Rabih et al. 2005. "Histone Acetylation by Trrap-Tip60 Modulates Loading of Repair Proteins and Repair
517 of DNA Double-Strand Breaks." *Nature Cell Biology* 8(1): 91–99.
518 ———. 2006. "Histone Acetylation by Trrap-Tip60 Modulates Loading of Repair Proteins and Repair of DNA
519 Double-Strand Breaks." *Nature Cell Biology* 8(1): 91–99.
520 Myler, Logan R et al. 2017. "Single-Molecule Imaging Reveals How Mre11-Rad50-Nbs1 Initiates DNA Break
521 Repair." *Molecular Cell* 67(5): 891–98.
522 Naidu, Samisubbu R., Alexander J. Lakhter, and Elliot J. Androphy. 2012. "PIASy-Mediated Tip60
523 Sumoylation Regulates P53-Induced Autophagy." *Cell Cycle* 11(14): 2717–28.
524 Noguchi, Chiaki et al. 2019. "The NuA4 Acetyltransferase and Histone H4 Acetylation Promote Replication
525 Recovery after Topoisomerase I-Poisoning." *Epigenetics and Chromatin* 12(1): 1–17.
526 https://doi.org/10.1186/s13072-019-0271-z.
527 Nugent, Rebecca L. et al. 2010. "Expression Profiling of S. Pombe Acetyltransferase Mutants Identifies
528 Redundant Pathways of Gene Regulation." *BMC Genomics* 11(1).
529 Onaka, Atsushi T. et al. 2016. "Rad51 and Rad54 Promote Noncrossover Recombination between Centromere
530 Repeats on the Same Chromatid to Prevent Isochromosome Formation." *Nucleic Acids Research* 44(22):
531 10744–57.
532 Ortega-Atienza, Sara et al. 2016. "ATM and KAT5 Safeguard Replicating Chromatin against Formaldehyde
533 Damage." *Nucleic Acids Research* 44(1): 198–209.
534 Osman, Fekret, Melissa Adriance, and Shirley McCready. 2000. "The Genetic Control of Spontaneous and UV-

535 Induced Mitotic Intrachromosomal Recombination in the Fission Yeast Schizosaccharomyces Pombe."
536 *Current Genetics* 38(3): 113–25.
537 Osman, Fekret, Elizabeth A. Fortunato, and Suresh Subramani. 1996. "Double-Strand Break-Induced Mitotic
538 Intrachromosomal Recombination in the Fission Yeast Schizosaccharomyces Pombe." *Genetics* 142(2):
539 341–57.
540 Papamichos-Chronakis, Manolis, Shinya Watanabe, Oliver J. Rando, and Craig L. Peterson. 2011. "Global
541 Regulation of H2A.Z Localization by the INO80 Chromatin-Remodeling Enzyme Is Essential for Genome
542 Integrity." *Cell* 144(2): 200–213. http://dx.doi.org/10.1016/j.cell.2010.12.021.
543 Pillus, Lorraine. 2008. "MYSTs Mark Chromatin for Chromosomal Functions." *Current Opinion in Cell*
544 *Biology* 20(3): 326–33.
545 Price, Brendan D., and Alan D. D'Andrea. 2013. "Chromatin Remodeling at DNA Double-Strand Breaks." *Cell*
546 152(6): 1344–54. http://dx.doi.org/10.1016/j.cell.2013.02.011.
547 Ransom, Monica, Briana K. Dennehey, and Jessica K. Tyler. 2010. "Chaperoning Histones during DNA
548 Replication and Repair." *Cell* 140(2): 183–95.
549 Renaud-Young, Margaret et al. 2015. "The NuA4 Complex Promotes Translesion Synthesis (TLS)-Mediated
550 DNA Damage Tolerance." *Genetics* 199(4): 1065–76.
551 Renaud, Emilie, Aurelia Barascu, and Filippo Rosselli. 2015. "Impaired TIP60-Mediated H4K16 Acetylation
552 Accounts for the Aberrant Chromatin Accumulation of 53BP1 and RAP80 in Fanconi Anemia Pathway-
553 Deficient Cells." *Nucleic Acids Research* 44(2): 648–56.
554 Rossetto, Dorine, Andrew W. Truman, Stephen J. Kron, and Jacques Côté. 2010. "Epigenetic Modifications in
555 Double-Strand Break DNA Damage Signaling and Repair." *Clinical Cancer Research*.
556 Sabatinos, Sarah A., and Susan L. Forsburg. 2010. "Molecular Genetics of Schizosaccharomyces Pombe."
557 *Methods in Enzymology* 470(C): 759–95.
558 Sapountzi, Vasileia, Ian R. Logan, and Craig N. Robson. 2006. "Cellular Functions of TIP60." *International*
559 *Journal of Biochemistry and Cell Biology* 38(9): 1496–1509.
560 Schindelin, Johannes et al. 2012. "Fiji: An Open-Source Platform for Biological-Image Analysis." *Nature*
561 *Methods*.
562 Schuchert, Peter, and Jurg Kohli. 1988. "The Ade6-M26 Mutation of Schizosaccharomyces Pombe Increases
563 the Frequency of Crossing Over." *Genetics* 119: 507–15.
564 Semer, M. et al. 2019. "DNA Repair Complex Licenses Acetylation of H2A.Z.1 by KAT2A during
565 Transcription." *Nature Chemical Biology* 15(10): 992–1000. http://dx.doi.org/10.1038/s41589-019-0354-y.
566 Shao, Zhengping et al. 2012. "Persistently Bound Ku at DNA Ends Attenuates DNA End Resection and
567 Homologous Recombination." *DNA Repair* 11(3): 310–16. http://dx.doi.org/10.1016/j.dnarep.2011.12.007.

568 Sharma, G. G. et al. 2010. “MOF and Histone H4 Acetylation at Lysine 16 Are Critical for DNA Damage
569 Response and Double-Strand Break Repair.” *Molecular and Cellular Biology* 30(14): 3582–95.
570 Shastri, Nishita et al. 2018. “Genome-Wide Identification of Structure-Forming Repeats as Principal Sites of
571 Fork Collapse upon ATR Inhibition.” *Molecular Cell* 72(2): 222-238.e11.
572 https://doi.org/10.1016/j.molcel.2018.08.047.
573 Shibata, Atsushi, Penny Jeggo, and Markus Löbrich. 2018. “The Pendulum of the Ku-Ku Clock.” *DNA Repair*
574 71(August): 164–71. https://doi.org/10.1016/j.dnarep.2018.08.020.
575 Smith, Edwin R. et al. 1998. “ESA1 Is a Histone Acetyltransferase That Is Essential for Growth in Yeast.” *Proc*
576 *Natl Acad Sci USA* 95(March): 3561–65.
577 Song, Suisui, Kelly E. McCann, and J. Martin Brown. 2008. “Radiosensitization of Yeast Cells by Inhibition of
578 Histone H4 Acetylation.” *Radiation Research*.
579 Soria, Gaston, Sophie E. Polo, and Geneviève Almouzni. 2012. “Prime, Repair, Restore: The Active Role of
580 Chromatin in the DNA Damage Response.” *Molecular Cell* 46(6): 722–34.
581 Stubbe, Joanne, and John W. Kozarich. 1987. “Mechanisms of Bleomycin-Induced DNA Degradation.”
582 *Chemical Reviews* 87(5): 1107–36.
583 Sun, Yingli et al. 2005. “A Role for the Tip60 Histone Acetyltransferase in the Acetylation and Activation of
584 ATM.” *Proceedings of the National Academy of Sciences of the United States of America* 102(37): 13182–
585 87. http://www.pnas.org/content/102/37/13182.full.
586 ———. 2009. “Histone H3 Methylation Links DNA Damage Detection to Activation of the Tumour
587 Suppressor Tip60.” *Nature Cell Biology* 11(11): 1376–82.
588 Syed, Aleem, and John A. Tainer. 2018. “The MRE11–RAD50–NBS1 Complex Conducts the Orchestration of
589 Damage Signaling and Outcomes to Stress in DNA Replication and Repair.” *Annual Review of*
590 *Biochemistry* 87(1): 263–94.
591 Sykes, Stephen M. et al. 2006. “Acetylation of the P53 DNA-Binding Domain Regulates Apoptosis Induction.”
592 *Molecular Cell* 24(6): 841–51.
593 Tamburini, B. A., and J. K. Tyler. 2005. “Localized Histone Acetylation and Deacetylation Triggered by the
594 Homologous Recombination Pathway of Double-Strand DNA Repair.” *Molecular and Cellular Biology*
595 25(12): 4903–13. http://mcb.asm.org/cgi/doi/10.1128/MCB.25.12.4903-4913.2005.
596 Tang, Jiangbo et al. 2013. “Acetylation Limits 53BP1 Association with Damaged Chromatin to Promote
597 Homologous Recombination.” *Nature Structural and Molecular Biology* 20(3): 317–25.
598 http://dx.doi.org/10.1038/nsmb.2499.
599 Tang, Yi, Jianyuan Luo, Wenzhu Zhang, and Wei Gu. 2006. “Tip60-Dependent Acetylation of P53 Modulates
600 the Decision between Cell-Cycle Arrest and Apoptosis.” *Molecular Cell* 24(6): 827–39.

601 Teixeira-Silva, Ana et al. 2017. "The End-Joining Factor Ku Acts in the End-Resection of Double Strand
602 Break-Free Arrested Replication Forks." *Nature Communications* 8(1). http://dx.doi.org/10.1038/s41467-
603 017-02144-5.
604 Thomas, Tim, and Anne K. Voss. 2007. "The Diverse Biological Roles of MYST Histone Acetyltransferase
605 Family Proteins." *Cell Cycle*.
606 Tomita, K. et al. 2003. "Competition between the Rad50 Complex and the Ku Heterodimer Reveals a Role for
607 Exol in Processing Double-Strand Break." *Molecular and Cellular Biology* 23(15): 5186–97.
608 Utley, R. T., and J. Côté. 2003. "The MYST Family of Histone Acetyltransferases." *Current Topics in*
609 *Microbiology and Immunology*.
610 Voss, Anne K., and Tim Thomas. 2009. "MYST Family Histone Acetyltransferases Take Center Stage in Stem
611 Cells and Development." *BioEssays*.
612 Walworth, Nancy C, and Rene Bernards. 1996. "Rad-Dependent Response of the Chk1-Encoded Protein Kinase
613 at the DNA Damage Checkpoint." *Science* 271(5247): 353–56.
614 Wan, S, H Capasso, and N C Walworth. 1999. "The Topoisomerase I Poison Camptothecin Generates a Chk1-
615 Dependent DNA Damage Checkpoint Signal in Fission Yeast." *Yeast (Chichester, England)* 15(10A):
616 821–28.
617 Xhemalce, Blerta, and Tony Kouzarides. 2010. "A Chromodomain Switch Mediated by Histone H3 Lys 4
618 Acetylation Regulates Heterochromatin Assembly." *Genes and Development* 24(7): 647–52.
619 Xu, Ye et al. 2010. "The P400 ATPase Regulates Nucleosome Stability and Chromatin Ubiquitination during
620 DNA Repair." *Journal of Cell Biology* 191(1): 31–43.
621 ———. 2012. "Histone H2A.Z Controls a Critical Chromatin Remodeling Step Required for DNA Double-
622 Strand Break Repair." *Molecular Cell* 48(5): 723–33.
623 Yu, Yang et al. 2013. "A Proteome-Wide Visual Screen Identifies Fission Yeast Proteins Localizing to DNA
624 Double-Strand Breaks." *DNA Repair* 12(6): 433–43. http://dx.doi.org/10.1016/j.dnarep.2013.04.001.
625 Zhou, B. O. et al. 2010. "SWR1 Complex Poises Heterochromatin Boundaries for Antisilencing Activity
626 Propagation." *Molecular and Cellular Biology* 30(10): 2391–2400.
627 http://mcb.asm.org/cgi/doi/10.1128/MCB.01106-09.
628 Zhu, Zhu et al. 2008. "Sgs1 Helicase and Two Nucleases Dna2 and Exo1 Resect DNA Double-Strand Break
629 Ends." *Cell* 134(6): 981–94.
630 Zlatanova, Jordanka, and Amit Thakar. 2008. "H2A.Z: View from the Top." *Structure* 16(2): 166–79.
631
632

633 **Figure Legends**

634 **Figure 1. *mst1-L344S* mutants are sensitive to the DSB-inducing agent bleomycin.** Cells were grown in YES
635 media overnight at 25ºC then 5X serial dilutions were spotted onto YES plates or YES plates containing
636 bleomycin. Plates were incubated at 25ºC and photographed after 4 days. 1 unit of bleomycin = 1 mg (by potency)

637 **Figure 2. The *mst1-L344S* allele affects DSB repair. A.** An assay to test chromosomal instability from (Osman,
638 Fortunato, and Subramani 1996). Two non-functional *ade6* alleles flank the functional *ura4+* gene. *the ade6-L469*
639 has a mutation at the C terminus while the *ade6-M26* allele has a mutation at the N-terminus (indicated by the
640 vertical lines). Several recombination outcomes are possible and are described in results and methods. **B.** Cells
641 were grown in YES media overnight at 25ºC then 5X serial dilutions were spotted onto YES (*HO* repressed) or
642 PMG without thiamine (*HO* induced). Plates were incubated at 25ºC and photographed after 5 days. **C**. Percent
643 of deletion, conversion and complex rearrangements after double strand break induction in WT and *mst1-L344S*
644 using the assay in **A**. The bold line in each box represents median and the filled circles represent outliers. Asterisks
645 indicate that recombination percentage is significantly different than WT ($p<0.05$, Mann-Whitney Test). **D**.
646 Chromatin immunoprecipitation assay to test recruitment of Mre11-myc, Rad52-YFP and Mst1-V5 to a single
647 DNA double strand break. Using a construct from (Du, Nakamura, and Russell 2006) one single double strand
648 break can be made with the *HO* endonuclease and protein interaction with chromatin can be monitored at 0.2, 2,
649 9 and 16Kb from the break. Following break induction, time points were taken at 0, 6, 8, 10, 12 and 14 hours.
650 Multiplex PCR was done with primers for all four positions from the break and with *act1+* primers (control).
651 Inset: Agarose gel electrophoresis showing banding patterns of PCR reactions. The intensity of each band was
652 normalized as (IP/Input)/(IP/Input actin) and graphed.

653 **Figure 3. The *mst1-L344S* mutant affects recruitment of repair proteins at 25ºC A. Top:** Percentage of cells
654 with RPA (Rad11) and Rad52 foci in WT, *mst1-L344S*, *pht1-4KR*, *pht1*Δ, *ku70*Δ and *ku70*Δ *mst1-L344S.* The
655 bold line in each box represents median and the filled circles represent outliers. Asterisks represent percentage of
656 cells with foci is significantly different than that in WT (*: $p<0.05$, **: $p<0.01$, Mann-Whitney Test) **Bottom:**
657 Examples of WT and *mst1-L344S* cells with Rad11 and Rad52 foci. Scale bar is 10µm. Rad11-CFP is colored
658 magenta for visibility. **B. Top:** Percentage of cells with Rad54 foci in WT and *mst1-L344S, pku70*Δ *and pku70*Δ
659 *mst1-L344S.* The bold line in each box represents median and the filled circles represent outliers. **Bottom:**
660 Examples of WT and *mst1-L344S* cells with Rad54 foci under phleomycin treatment. Scale bar is 10µm. **C. Left:**
661 Percentage of cells with colocalized Rad52-CFP and HO-induced mCherry foci over 240 minutes. **Right:**
662 Representatives of WT and *mst1-L344S* cells with Rad52-CFP and HO-induced mCherry foci over time. Rad52-
663 CFP is colored green for visibility. **D.** Percentage of cells with mCherry-LacI signal over 240 minutes. Image was
664 taken every 8 min in wild-type and *mst1-L344S*, and every 48 min in other mutants.

665 **Figure 4. Mst1 affects DNA lesion repair but does not affect checkpoint activation. A. Left:** Percentage of
666 cells with RPA (Rad11) and Rad52 foci in WT and *mst1-L344S* after CPT and MMS treatments. The bold line in
667 each box represents median and the filled circles represent outliers. **Right:** examples of WT and *mst1-L344S* cells
668 with RPA and Rad52 foci after drug treatment. Scale bar is 10µm. Rad11-CFP is colored magenta for visibility.
669 **B**. Phosphorylation of Chk1-HA is not affected in *mst1-L344S* after treatment of cells with three types of DNA
670 damaging agents at 32°C. cells were treated for 4 hours with 0.01% MMS, 15mM HU or 40µM CPT and the and
671 the Chk1-HA phosphorylation shift band was detected by Western blotting with 12CA5 anti-HA antibody. **C**.
672 H2A phosphorylation dynamics are not affected in *mst1-L344S* when cells are treated with 40µM CPT. Western
673 Blot with an anti-phosphorylated H2A antibody showing that phosphorylation of H2A peaks 4 hours after
674 treatment with drug then the signal is down regulated 4 hours post drug removal. *hta1-S129A:* control non-
675 phosphorylatable form of H2A; α-PCNA: control antibody.
676 **Figure 5. Model for the function of Mst1 in DSB repair.** Mst1 facilitates HR by promoting long-range resection
677 and inhibiting Ku70-associated mechanism that inhibits HR. Such function is accomplished by acetylating H2A.Z
678 and thus promoting the turnover of H2A.Z at the DSB. Therefore, the histone variant can no longer block the
679 break site. The removal of H2A.Z allows Exo1 to access the break and thus promotes downstream recombination-
680 mediated repair.
681 **Supplementary Figure S1**. **Examples of cells with RPA (Rad11), Rad52, Rad54, Mre11 and pKu70 foci**
682 **after treatment with phleomycin at 25ºC**. **A.** Rad11-CFP and Rad52-YFP foci in *pku70Δ* and *pku70Δmst1-*
683 *L344S*. **B.** Rad11-CFP and Rad52-YFP foci in *pht1-4KR* and *pku70Δ*. **C.** Rad54-GFP foci in *pku70Δ* and
684 *pku70Δmst1-L344S*. **D.** pKu70-YFP foci in pht1-4KR and *pht1Δ*. No drug = untreated controls.
685 **Supplementary Figure S2. *pku70*Δ does not affect cell length at septation in *mst1-L344S* at 25ºC.** Length at
686 septation at 25ºC of WT, *mst1-L344S*, *pku70*Δ, and *pku70*Δ *mst1-L334S* cells. The bold line in each box represents
687 median and the filled circles represent outliers.
688 **Supplementary Figure S3. *mst1-L344S* interacts genetically with genes in the checkpoint pathways.** Cells
689 were grown in YES media overnight at 32ºC then 5X serial dilutions were spotted onto YES plate or YES plates
690 containing the indicated drugs. Plates were incubated at 32ºC and photographed after 4 days.
691
692
693
694
695

Figure 1. ***mst1-L344S*** **mutants are sensitive to the DSB-inducing agent bleomycin.**

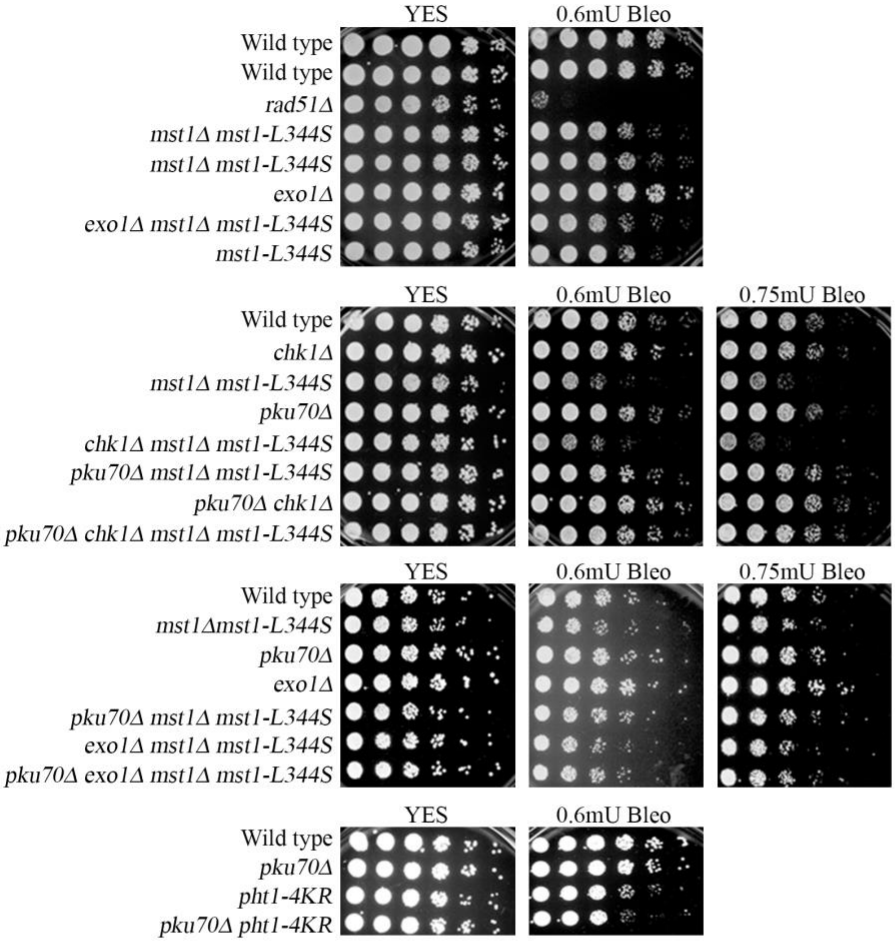

696

Figure 2. The *mst1-L344S* allele affects DSB repair.

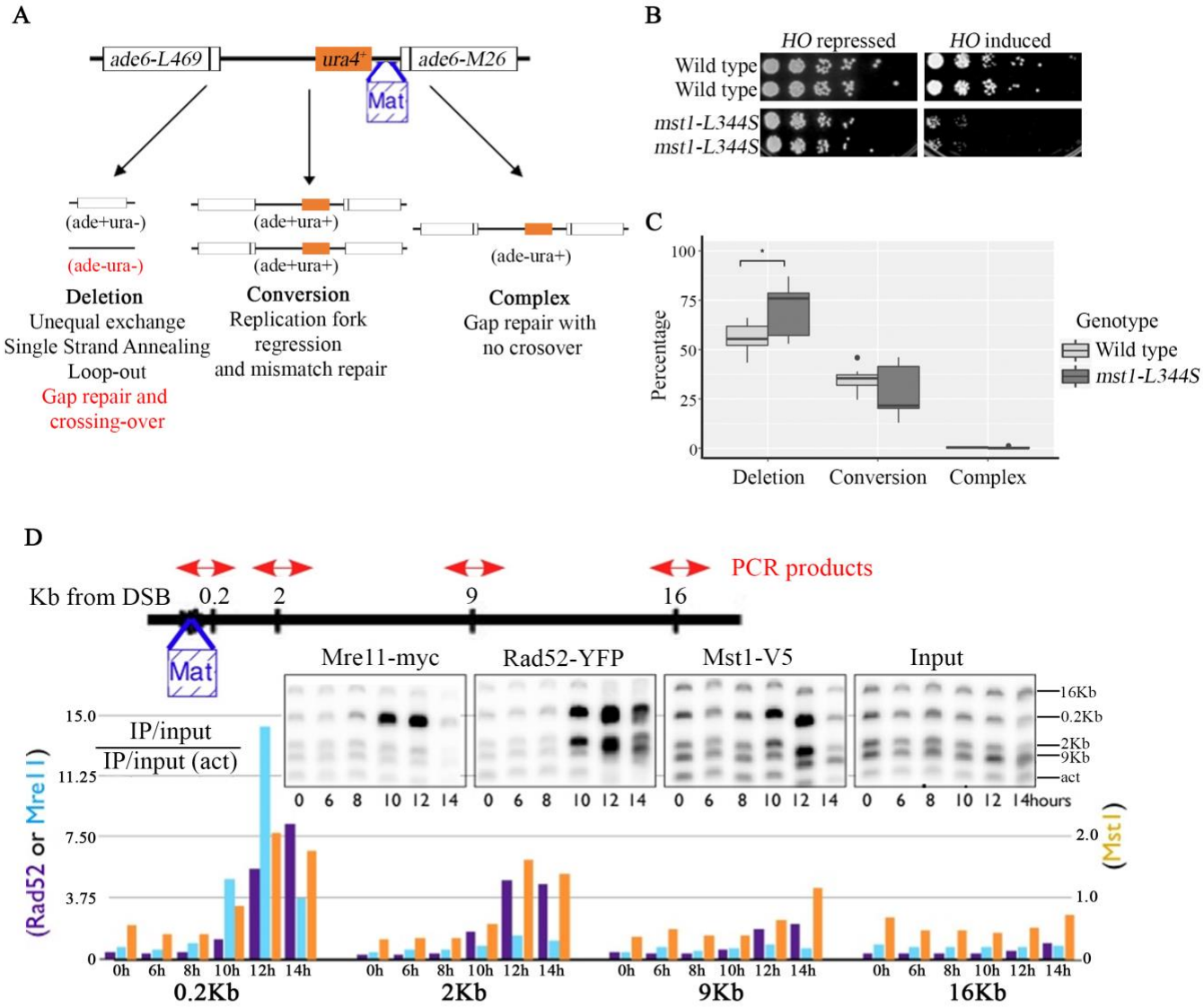

697

Figure 3. The *mst1-L344S* mutant affects recruitment of repair proteins.

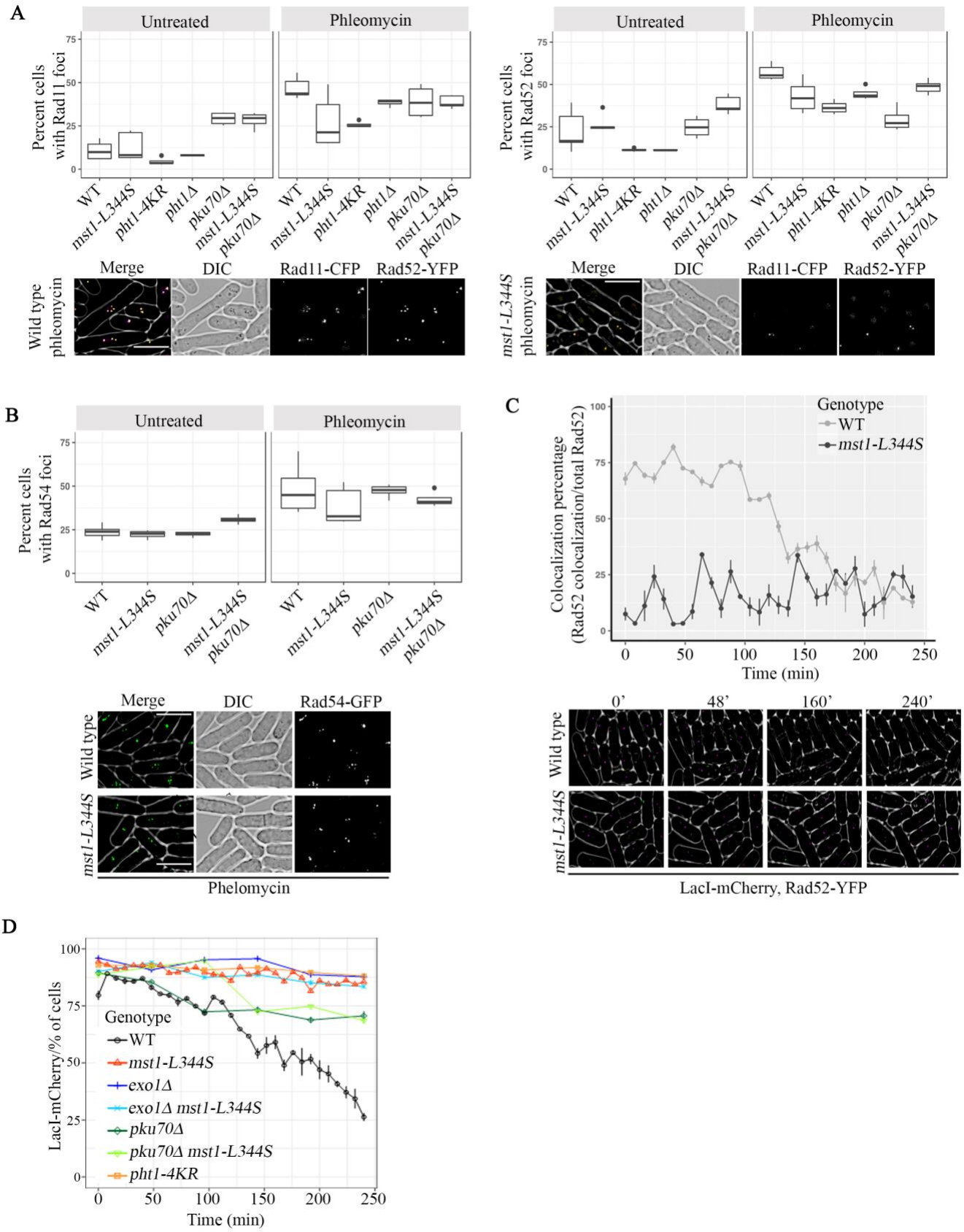

698

Figure 4. Mst1 affects DNA lesion repair but does not affect checkpoint activation.

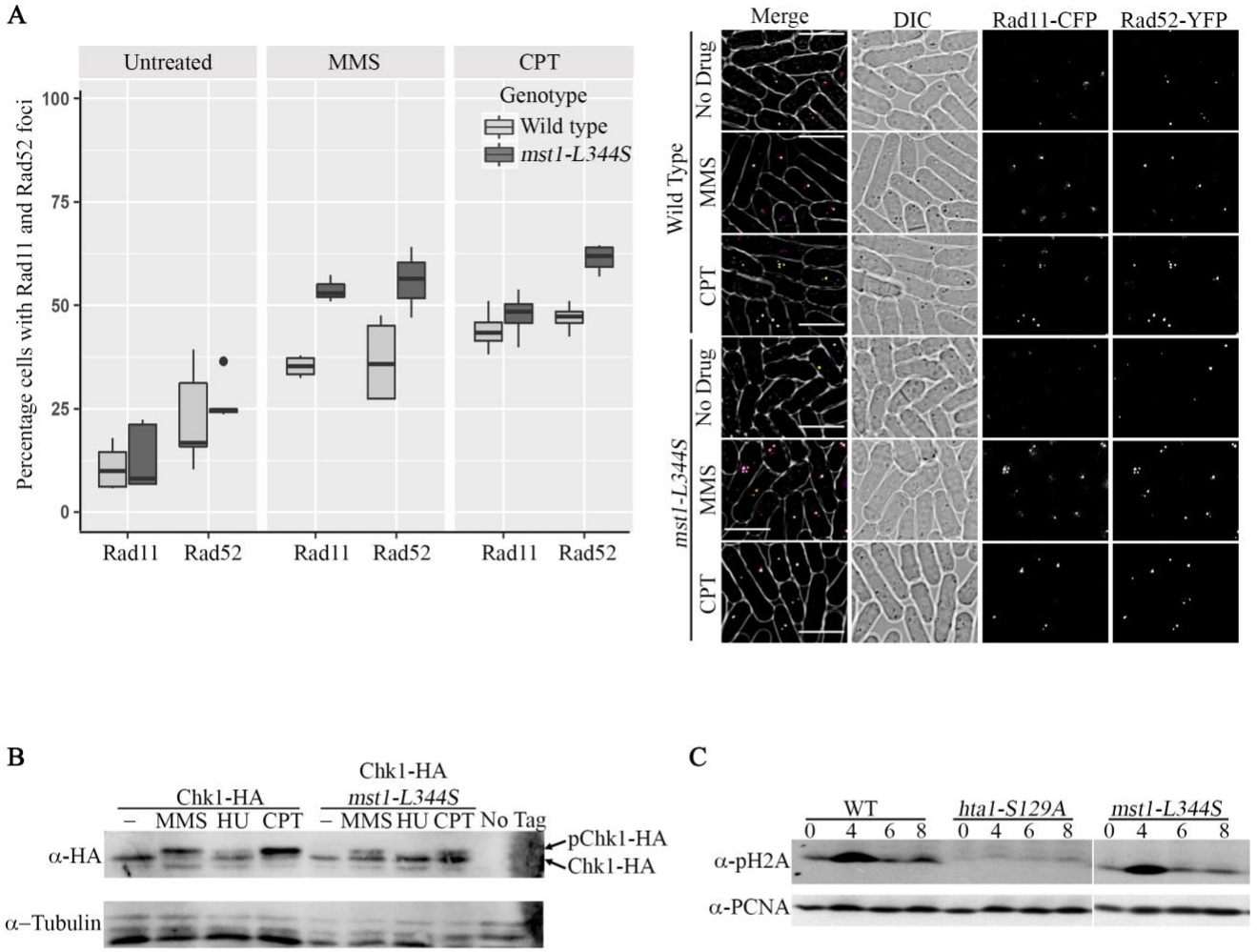

699

Figure 5. Model for the function of Mst1

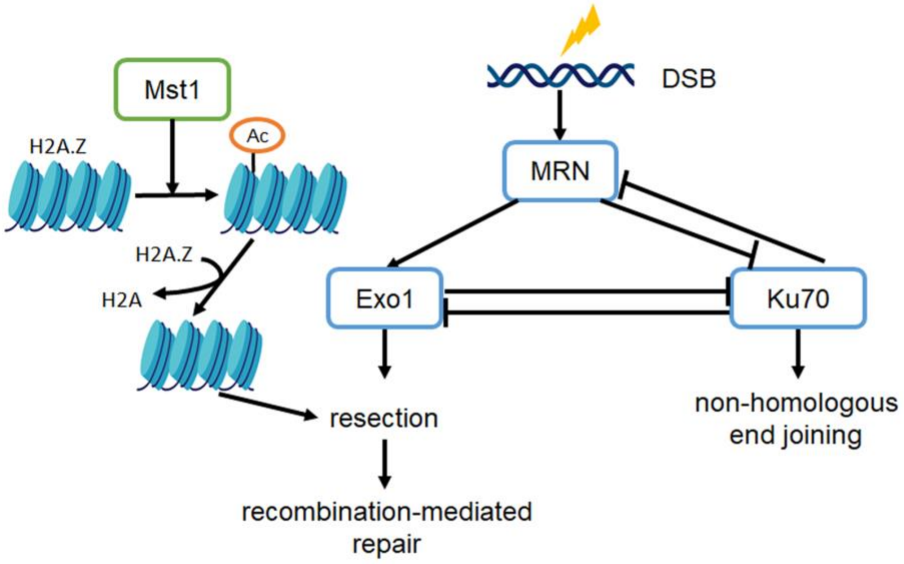

700